Water Research 253 (2024) 121284

Contents lists available at ScienceDirect

Water Research

journal homepage: www.elsevier.com/locate/watres

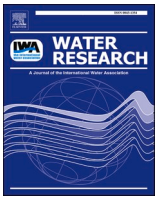

Do baseline assumptions alter the efficacy of green stormwater infrastructure to reduce combined sewer overflows?

Mayra Rodriguez [a], Giovan Battista Cavadini [a,b], Lauren M. Cook [a,*]

[a] Department of Urban Water Management, Swiss Federal Institute for Aquatic Research, Dübendorf, Switzerland
[b] Institute of Environmental Engineering, ETH Zürich, Switzerland

ARTICLE INFO

Keywords:
Combined sewer systems
Evapotranspiration
Modeling assumptions
Groundwater
SWMM

ABSTRACT

Green stormwater infrastructure (GSI) is growing in popularity to reduce combined sewer overflows (CSOs) and hydrologic simulation models are a tool to assess their reduction potential. Given the numerous and interacting water flows that contribute to CSOs, such as evapotranspiration (ET) and groundwater (GW), these models should ideally account for them. However, due to the complexity, simplified models are often used, and it is currently unknown how these assumptions affect estimates of CSOs, GSI effectiveness, and ultimately planning guidance. This study evaluates the effect on estimates of CSOs and GSI effectiveness when different flows and hydrologic processes are neglected. We modified an existing EPA SWMM model of a combined sewer system in Switzerland to include ET, GW, and upstream inflows. Historical rainfall data over 30 years are used to assess volume and duration of CSOs with and without three types of GSI (bioretention basins, permeable pavements and green roofs). Results demonstrate that neglect of certain flows in modelling can alter CSO volumes from -15 % to 40 %. GSI effectiveness also varies considerably, resulting in differences in simulated percent of CSO volume reduced from 8 % to 35 %, depending on the GSI type and modeled flow or process. Representation of GW within models is particularly crucial when infiltrating GSI are present, as CSOs could increase in certain subcatchments due to higher GW levels from increased infiltration. When basing GSI planning decisions on modeled estimates of CSOs, all relevant hydrologic processes should be included to the extent possible, and uncertainty and assumptions should always be considered.

1. Introduction

Combined sewer systems are designed to collect both sewage and stormwater in the same pipe network and convey it to wastewater treatment plants (WWTPs) (Butler et al., 2018). When the amount of stormwater entering the pipes exceeds the system capacity, untreated wastewater is discharged into receiving waters (Balmforth, 1990). These discharges, referred to as Combined Sewer Overflows (CSOs), are one of the main causes of urban water pollution (Copetti et al., 2019) and many cities and governments worldwide are under pressure to reduce or eliminate them (Environment Agency and Department for Environment, 2022; U.S.C 2020). Green stormwater infrastructure (GSI), such as bioretention basins, rain gardens, green roofs and permeable pavement, is gaining popularity as a measure to reduce CSOs (Fischbach et al., 2017; Fu et al., 2019; Roseboro et al., 2021) because these systems retain, infiltrate, and evaporate stormwater before it reaches the sewer (Almaaitah et al., 2021), are cost-effective (Browder et al., 2019; Matsler et al., 2021), and provide numerous environmental and social benefits (Chatzimentor et al., 2020; Cook and Larsen, 2021).

To effectively plan for reduction measures, cities must first characterise the volume, duration, and frequency of CSOs entering adjacent receiving waters and then estimate the coverage of GSI needed to achieve desired reductions. Since CSOs are rarely measured due to logistic difficulties of in-sewer devices (Passerat et al., 2011), hydrologic simulation models, such as the EPA Storm Water Management Model (SWMM) (Rossman, 2015), MIKE (DHI 2023), and InfoWorks ICM (Innovyze 2014), are typically used to estimate CSOs (Niazi et al., 2017). These discharges are, however, notoriously difficult to simulate as there are numerous water flows that can affect water level within the combined system, including wastewater, stormwater, groundwater (GW), and other inflows (from upstream catchments, for instance). Evapotranspiration may also play a role, as it can alter stormwater flows, particularly when GSI are present (Ebrahimian et al., 2019). To calculate these flows and set up the model, ample information about the combined

* Corresponding author at: Eawag, Überlandstr. 133, 8600 Dübendorf, Switzerland.
E-mail address: Lauren.Cook@eawag.ch (L.M. Cook).

https://doi.org/10.1016/j.watres.2024.121284
Received 19 June 2023; Received in revised form 6 December 2023; Accepted 5 February 2024
Available online 6 February 2024

system and surrounding catchment must be determined (e.g., number and size of pipes, land cover, etc.), which often requires coordination with local municipalities (Blumensaat et al., 2023).

These simulation models thus range in complexity, assumptions, and structure, which could significantly influence the conclusions of the analysis, including the surface area of GSI needed to reduce CSO discharges and in consequence, the costs involved (Broekhuizen et al., 2019; Casal-Campos et al., 2015). GSI effectiveness against CSOs varies considerably among studies and catchments (Fu et al., 2019; Jean et al., 2022; Joshi et al., 2021; Roseboro et al., 2021; Torres et al., 2021). Some studies find that GSI can reduce CSO volume by more than 90 % (Jean et al., 2022; Joshi et al., 2021), outperforming traditional storage tanks (Joshi et al., 2021). However, other studies show that CSO volumes would be reduced by less than 20 % (Fischbach et al., 2017; Roseboro et al., 2021) and additional grey infrastructure would still be required to fully eliminate CSOs, especially given expected increases in rainfall intensity due to climate change (Casal-Campos et al., 2015; Roseboro et al., 2021). Parameter uncertainty of catchment characteristics (e.g., terrain, rainfall, imperviousness, sewer system design, climate, GSI placement) (Hung et al., 2020) and GSI characteristics (e.g., implementation area, infrastructure type, soil type, etc.) (Leimgruber et al., 2018) contribute to this variability. However, assumptions related to water flows and processes (such as ET and GW), as well as, equations, numerical methods, and boundary conditions (Deletic et al., 2012) also play a role. For instance, the two studies that have accounted for feedbacks between GSI and the GW table (albeit at a smaller scale) found that this more realistic representation improved the model accuracy of bioretention basin simulations (Zhang et al., 2018) (in one study by as much as 14.7 % (Kim et al., 2019)). Another study found that including shading and ET in hydrologic simulation models reduced the error of simulated outflows from green roofs by 18 % (Hörnschemeyer et al., 2021). External inputs to the sewer system, such as infiltration and inflows (I&I) or direct connections from other drainage areas, are also relevant for estimating sewer flows (Staufer et al., 2012; Weiß et al., 2002). For instance, (Cook et al., 2018) found that average sewer flows could nearly double when I&I are considered. Ultimately, when contributing flows and processes are poorly represented, so are CSOs, and the required GSI to reduce them.

Despite this evidence, many studies neglect GW and ET, as well as, other external inputs to the sewer system in their modelled representation of combined sewers (e.g., Joshi et al. (2021) and, Wang et al. (2017)). This is understandable, as it may not be feasible or worthwhile to include every detail in every case study. However, to date, there are no studies that have evaluated the individual nor the combined effect of all contributing flows (e.g., GW, ET, and external inflows) on CSOs at a catchment scale. Inaccurate estimations of CSOs and resulting GSI effectiveness could lead to improper planning and underestimation of costs, however, increased complexity takes time and effort. More information is needed to make an informed decision about how accurately reality should be represented when evaluating the effectiveness of GSI for combined sewer systems.

The goal of this study is to evaluate how estimations of CSO discharges, and the effectiveness of green stormwater infrastructure to reduce these discharges, are affected when hydrologic simulations neglect real-world flow conditions. We evaluate the effects of three flows, groundwater (GW), evapotranspiration (ET), and boundary inflows (BI) from an upstream catchment, on CSOs without GSI, as well as, with three types of GSI, including bioretention basins, permeable pavements and green roofs. This study will set the stage to determine how accurate reality must be represented in combined sewer system models in order to accurately assess GSI requirements. It will inform engineers and planners about the importance of including these different flows in their models, as well as, the expected range and uncertainty in estimations of CSOs and GSI effectiveness when they are excluded.

2. Methods and data

The EPA Storm Water Management Model (SWMM) is used to test how an accurate representation of all hydrological processes and water flows affects simulated estimates of CSOs and the ability of GSI to reduce them. SWMM is a hydrologic and hydraulic model widely used for long-term, continuous simulation of stormwater runoff, drainage and sewer systems, as well as, GSI (Rossman, 2015).

As shown in Fig. 1, the original model, described in Joshi et al. (2021) (not used in this study), underwent minor updates (to the imperviousness and infiltration scheme; see Section 2.1) and is herein referred to as the base case model (BC). The BC model simplifies or excludes BI, ET, and GW during simulation (as in Joshi et al. (2021)) and is used for comparison to simulations that individually include these flows (BI, ET, and GW model simulations shown in Fig. 1 and described in Section 2.2). The combined model (CB) integrates BI, ET, and GW during simulation and is also compared to the BC model (see Section 2.2). The BC and CB models are both calibrated and validated in this study (*calibration 1* and *2*, respectively, in Section 2.3). All model versions are first simulated without GSI elements to represent baseline CSO conditions and then with three types of GSI: bioretention basins (*bb*), permeable pavements (*pp*), and green roofs (*gr*) (Section 2.4). CSOs are quantified at the system level (by summing the discharge from six outfalls; see Section 2.1) using the total annual volume, the duration (hours per year), and the frequency (days per year). A CSO event is classified as discharge that exceeds 0.01 m^3h^{-1}.

2.1. Base case (BC) simulation model

In this study, the BC SWMM model is based on the combined sewer system (CSS) of a 7000-inhabitant catchment, Fehraltorf, located 15 km east of Zurich, Switzerland (Federal Office for Statistics, 2022; Keller, 2016). This real-world CSS carries sewage from Fehraltorf and two neighbouring municipalities (Rumlikon and Russikon, as shown in Fig. 2) to the WWTP (max. capacity: 180 Ls^{-1}). Six CSO outflows (shown in green in Fig. 2) are active in most rainfall events and GW infiltration can represent between 15 % and 40 % of the dry weather flows arriving at the WWTP (Hadengue et al., 2021; Krejci et al., 1994). Thus, groundwater infiltration into the pipes is expected to be high (Keller, 2016; Ramgraber et al., 2021).

The original SWMM model, developed by Keller (Keller, 2016) and later updated by Joshi et al. (Joshi et al., 2021), includes 246 subcatchments (95.1 hectares) that are connected to the CSS (shown in Fig. 2 in purple), with 427 manholes (i.e., nodes in SWMM), 430 sewer pipes (i.e., links in SWMM), six CSO outfalls (RUB 40a, RUB 48b, RUB 59, RUB 128, and SK 102; shown in Fig. 2), and five storage tanks (not shown). In the original model, infiltration was modelled using a Hortonian approach (Rossman and Huber, 2016), while ET was considered as constant monthly rates, albeit with potential for oversimplification (Bai et al., 2015). Measured boundary inflows (from 2016 – 2018; available in the Urban Water Observatory dataset (Blumensaat et al., 2023)) were used for calibration only. GW was included in calibration and simulation as constant inflows into the nodes, calculated based on a night-minimum flow analysis within the catchment (see Hadengue et al. (2021), who developed this approach). This model lacks explicit GW dynamic modelling, and does not account for the interaction with other hydrological processes in the catchment (see Joshi et al. (2021) for more information on this version).

In this study, minor updates are made to the imperviousness and infiltration equations of the original model, henceforth referred to as the base case (BC) model. Subcatchment percent imperviousness is computed using recent data acquisitions of land cover categories provided by the municipality of Fehraltorf (Blumensaat et al., 2023). The infiltration model is updated to the Green-Ampt model, chosen for its ability to account for soil moisture between rain events, and therefore advantageous for continuous simulation (Rossman, 2015; Zhang et al.,

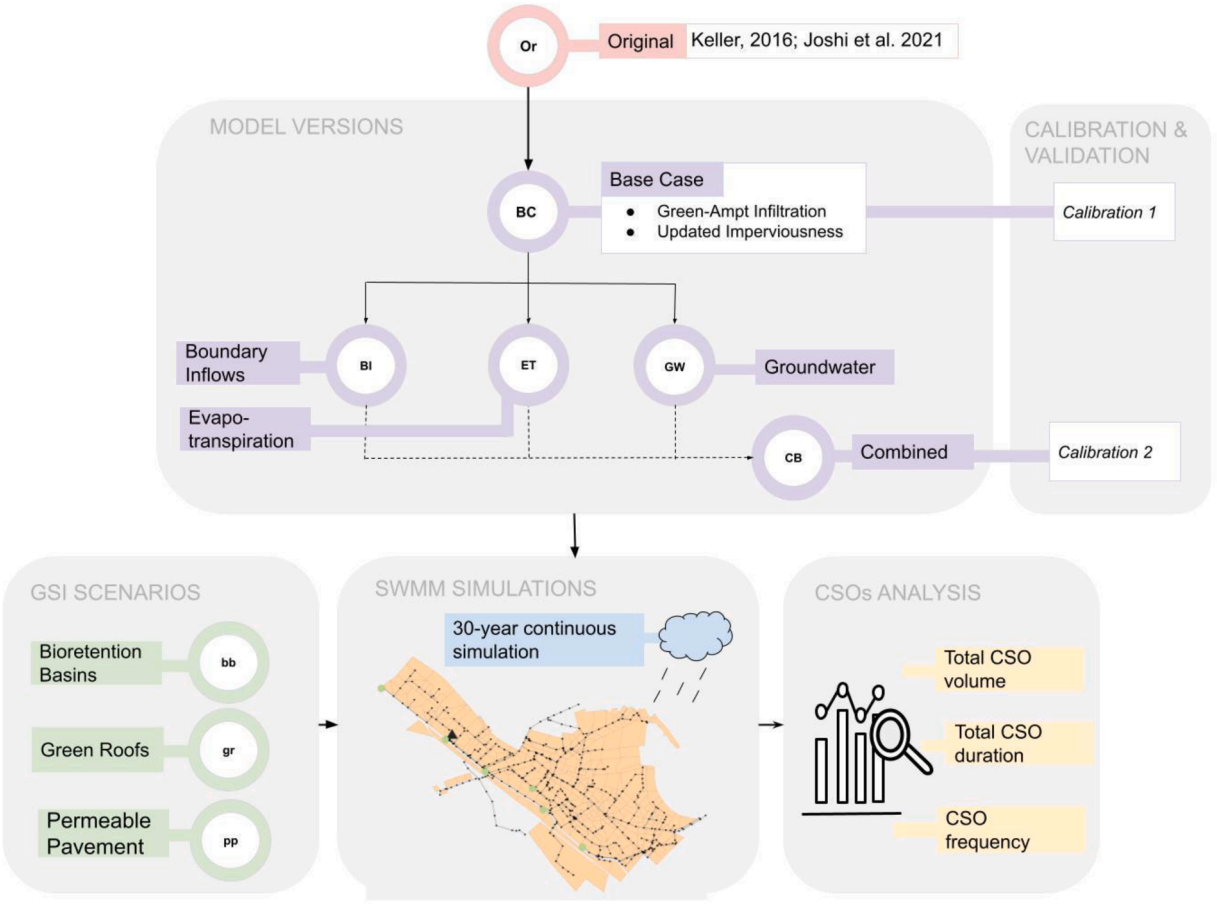

Fig. 1. Summary of the components of this study: model versions and their calibration and validation, simulated in SWMM, both with and without GSI scenarios, then compared by quantifying CSO volume, duration, and frequency from each simulation.

2018).

The BC model is calibrated in a consistent manner with the original model, apart from ET (explained in Section 2.3; see *calibration 1*), where BI are included as measured data, GW provided as estimated inflows, and ET as a timeseries. The BC model is simulated over 30 years without BI, GW, and ET to act as a reference case for the other model versions (**see** Section 2.2).

2.2. Model versions

The calibrated BC model presented in Section 2.1 is used for comparison to evaluate how more explicit consideration of ET, BI, and GW and their interactions affect simulated estimates of CSO discharge and GSI performance. Presented in the following sub-sections, these factors are first assessed individually by updating the BC model to more accurately represent ET (Section 2.2.1), BI (Section 2.2.2), and GW (Section 2.2.3). These factors are then assessed altogether within a combined (CB) model (Section 2.2.3) that is recalibrated (see Section 2.3).

2.2.1. Evapotranspiration (ET)

In the ET model version, evapotranspiration is input into the base case model as a user-defined time series of daily values instead of constant monthly values (as in Joshi et al. (2021)). This time series, obtained from MeteoSwiss for the Kloten weather station, is reference ET during the period January 1990–2020, derived from temperature, global radiation, humidity and wind measurements without consideration of vegetation and crop characteristics (Calanca et al., 2011). An average crop coefficient for the catchment could be included to reduce ET values in line with expected vegetation characteristics of the subcatchments (Allen et al., 1998). However, this value is likely close to one (as reported in De-Ville and Stovin (2023)). Reference ET thus constitutes a best-case scenario in terms of evapotranspiration rates, enabling investigation of the maximum potential impact of ET on CSOs and serving as a standard for other studies. It is worth noting that in SWMM, evaporation occurs from both impervious and pervious areas, as long as there is water on the surface of the subcatchments to evaporate.

2.2.2. Boundary inflows (BI)

The BI model version includes boundary inflows from the upstream catchments of Rumlikon and Russikon (see Fig. 2), over the 30-year simulation period, as opposed to Joshi et al. (2021) where they are ignored. These flows are estimated using a multi-layer perceptron (MLP) machine learning model (Scikit-Learn Developers, 2014), which was selected because it can learn complex nonlinear relationships between input variables and output variables (Maier and Dandy, 2000). Two MLP models were developed (one for each boundary inflow) using rainfall and flow measurements collected between 2016 and 2022 as part of the UWO project (Blumensaat et al., 2021; Figueroa et al., 2021; Keller, 2016). The MLP models performed satisfactorily for the calibration period, with an r^2 of 0.69 for Rumlikon, and 0.51 for Russikon. These values are considered acceptable for this study, as the flow trends are generally well-defined, yet slightly overestimated, representing a conservative estimate of boundary inflows. Further information on the model development and performance can be found in **SI S2**.

2.2.3. Groundwater (GW)

Due to its relevance in the Fehraltorf system, the GW model structure explicitly models GW using modules available in SWMM, instead of the

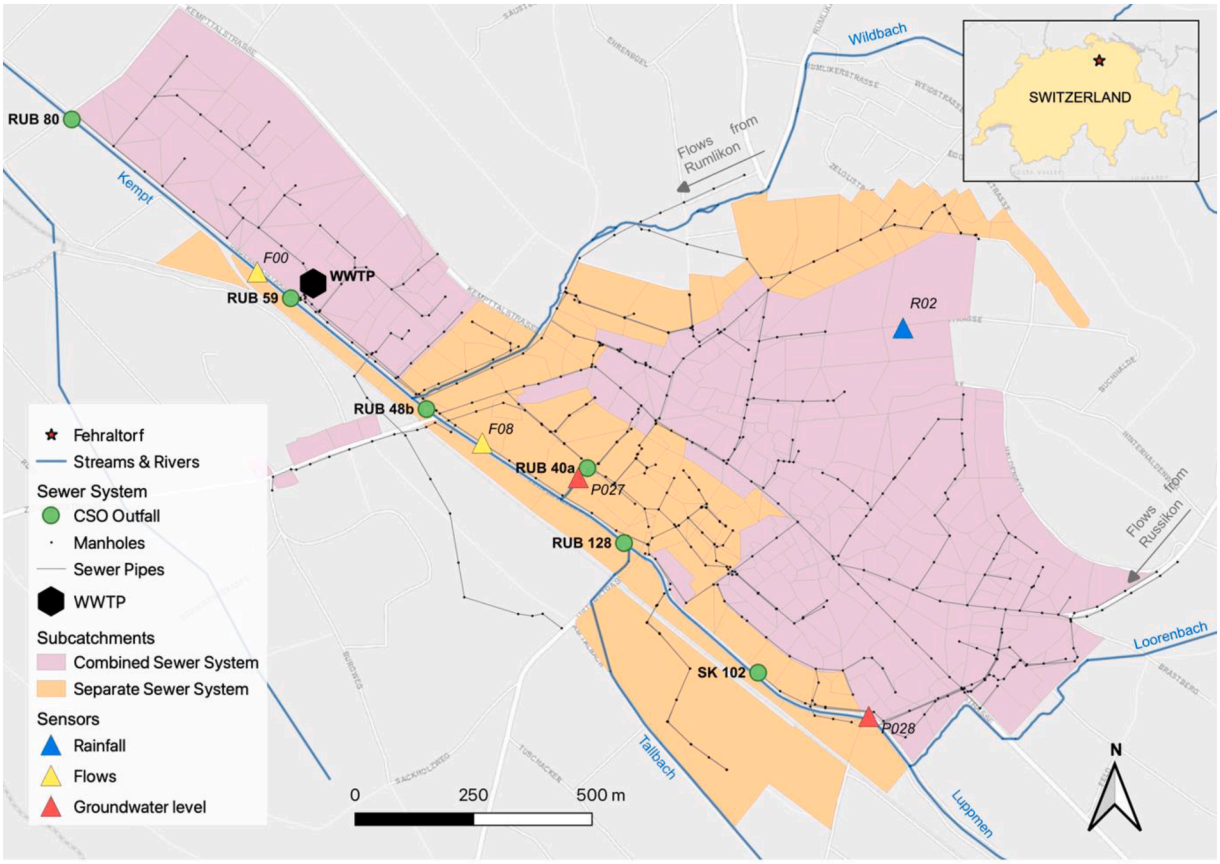

Fig. 2. Overview of the Fehraltorf sewer system (Section 2.1) and the sensors used for model calibration (Section 2.3). Information on the sensors and the data used is presented in the supplementary information (SI S1). Note: water from the sewer catchment is conveyed towards the wastewater treatment plant (WWTP), while the Luppmen creek flows from South-East to North-West.

calculated flows evenly distributed across the nodes (Hadengue et al., 2021). SWMM can simulate subsurface flows, including the release of GW from a subcatchment, percolation out of a GSI storage unit, and inflow and infiltration (Rossman and Huber, 2016; Zhang and Chui, 2020). However, some GW dynamics are simplified, including the feedback with GSI elements and spatial lumping of GW flows (further explained in **SI S3**). Despite these shortcomings, the addition of GW modules in the SWMM model is a step forward to evaluate the interactions between GW, GSI and the CSS. The parametrisation of the SWMM GW modules is determined by automatic calibration in the combined model, as described in Section 2.3. The GW model is simulated without BI and ET.

2.2.4. Combined (CB)

The combined model is calibrated (see Section 2.3, *calibration 2*) after GW modules are included. The CB model is simulated with statistically generated BI (Section 2.2.2), ET as a timeseries (Section 2.2.1), and with fully calibrated GW modules in SWMM, allowing for interactions between the GSI, sewer system, and the GW.

2.2.5. Simulation and comparison of all model versions

After calibration, all model versions are simulated in pyswmm (McDonnell et al., 2020) using 30-years of 10-minute rainfall data between January 1, 1990 and January 1, 2020 from a weather station in Kloten (15-km west of Fehraltorf) (MeteoSwiss, 2017). The parameters (e.g., land use) of the model were maintained constant throughout 30-year period. While we acknowledge that this assumption simplifies the real-world dynamics, it allows for a better comparison of the modelled flows under investigation.

To determine if the differences between the model versions are statistically significant, a dependent *t*-test for paired samples is performed on the model outputs (CSO volume, duration and frequency), using the Scipy python package (The SciPy Community 2023). The results are not considered significantly different if the p-value exceeds the confidence interval of 0.01, commonly used in the literature (Freedman et al., 2007). A further description of the *t*-test is available in **SI S7**.

2.3. Model calibration and validation

Due to a lack of field data for certain parameters, the BC model and the CB model are both automatically calibrated using a multi-objective evolutionary algorithm, NSGA-II (Deb et al., 2002). Four surface parameters are calibrated in the BC model (named *calibration 1*), while twelve parameters are calibrated in the GW model version, including soil porosity and seepage rate into deep groundwater (named *calibration 2*); see **SI S4** for a list of parameters and ranges. Flow and groundwater data from the Urban Water Observatory is used for the calibration and validation (Blumensaat et al., 2023). Further information on the sensors (shown in Fig. 2) and measurement data can be found in **SI S1**.

2.3.1. Automatic calibrations using evolutionary algorithms

The multi-objective evolutionary algorithm used for calibration, NSGA-II (Deb et al., 2002), was implemented in Python with the package Pymoo (Blank and Deb, 2020). The optimisation problem in Pymoo is formulated as follows,

$$Minimize: \ f_1(\vec{x}), f_2(\vec{x}), \ldots, f_n(\vec{x}) \tag{1}$$

$$\vec{x} \in \left[\vec{x}_{min}, \ \vec{x}_{max}\right] \tag{2}$$

where $\vec{x}$ is the vector of the parameters to be optimised and $\vec{x}_{min}$ and $\vec{x}_{max}$ are the lower and upper bounds of $\vec{x}$, respectively $f_1(\vec{x}), f_2(\vec{x}), \ldots, f_n(\vec{x})$ are the objective functions of $\vec{x}$, which determine the goodness-of-fit of the model. In this study, $\vec{x}$ corresponds to the subarea module parameters for *calibration 1* and the GW module parameters for *calibration 2* (see **SI S4**).

For *calibration 1*, two objective functions are minimized using data from two flow measurements in the main collector in the Fehraltorf system (Luppmenstrasse and WWTP, marked in Fig. 2 as F08 and F00, respectively), using a modified version of the Nash Sutcliffe Efficiency (NSE) coefficient.

Due to the characteristics of the problem definition in Pymoo, optimisation needs to be reformulated as a minimisation problem. Thus, the objective functions are defined as 1-NNSE (see **SI S3**), where the NNSE is the normalised NSE (Eq. (3)). Since the lower limit of the NSE is -∞, the NNSE is used to eliminate plausible issues during calibration.

$$NNSE = \frac{1}{2 - NSE} \tag{3}$$

The NNSE allows to re-scale the range between zero and one (NSE of one corresponds to an NNSE of one; NSE of zero to an NNSE of 0.5; and NSE of -∞ to an NNSE of zero). The same objective functions are used for *calibration 2*, with the addition of two objectives related to GW: the root mean square error (RMSE) between two GW-level measurements (shown in Fig. 2) and their respective simulations. Using multiple objective functions allows for spatially differentiated evidence of the model's ability to reflect the dynamics of a real-world sewer network.

The calibration was performed using the one-year period from 1st May 2018 to 30th April 2019. For *calibrations 1* and *2*, boundary inflows from the two neighbouring municipalities were supplied to the model as time series inputs (limited to the available observed data from UWO) and ET was supplied as a time series provided by MeteoSwiss with daily resolution (see Section 2.2.1 for more information). For *calibration 1* (BC model), GW was included as estimated inflows into the nodes (see Hadengue et al. (2021)), while for *calibration 2* (CB model), the SWMM groundwater module was enabled and also calibrated.

For the validation, the calibrated models were simulated during the one-year period from 1st May 2019 to 30th April 2020. In the validation process, the RMSE and the NSE were calculated for the different calibration locations. A description of the optimisation characteristics used, as well as, the selection of the final BC and CB parameters obtained from the last generation of the evolutionary optimisation can be found in **SI S4**.

2.4. Green stormwater infrastructure scenarios

This study considers three GSI elements, bioretention basins (*bb*), permeable pavements (*pp*), and green roofs (*gr*), which are implemented on different land cover types (e.g., rooftops, parking lots, grass), thus maximising their potential for implementation in urban areas (Joshi et al., 2021; Li et al., 2019; Wang et al., 2019).

Each GSI element is implemented to the same spatial extent, 10.8 % of the catchment or 103,082 m^2, which is equivalent to the maximum spatial extent for the green roofs (representing the area of all available flat roofs). The *bb* replace existing pervious areas in each subcatchment, while *pp* are installed in impervious areas that are not buildings or main roads (e.g., streets, pedestrian paths, and car parks) and *gr* on flat roofs. Pervious areas, impervious areas and flat roofs in each subcatchment are determined according to the existing land use types in Fehraltorf (obtained from the municipality; see **SI S5** for further information).

Runoff from impervious areas is routed to *bb*, while the other GSI only treat rainwater falling on their surface area, mimicking common GSI designs (Philadelphia Water Department 2023). Each GSI type is added individually to the catchment, resulting in three GSI scenarios. Although the total GSI area is equal in all scenarios (allowing for equal performance comparison among the scenarios), the resulting spatial distribution for each GSI element differs depending on the land use type in each subcatchment. The width of each GSI unit is calculated as the square root of the subcatchment area, to have a standard assumption for each subcatchment and avoid discrepancies in performance.

GSI parameters for SWMM were obtained from the literature (Joshi et al., 2021; Rossman and Huber, 2016; Wang et al., 2019) with relevant parameters summarised in Table 1 and the remainder shown in **SI S5**. The parameters are assumed to remain constant throughout the 30-year evaluation period.

3. Results and discussion

3.1. Model calibration and validation

The model calibration and validation results for the BC and CB models are summarised in Fig. 3, which compares the empirical cumulative distribution curves of the observed and simulated flows for two points in the main collector (Luppmenstrasse and WWTP, F00 and F08 respectively in Fig. 2). The tables in each graph show the NSE coefficients for each model version at that measured location.

The simulated flows at the WWTP match the observations well, which is confirmed by the high NSE values (over 0.5, which is a level considered acceptable in hydrological modelling practices (Moriasi et al., 2007)). The largest differences between the simulated and observed flow at the WWTP are for flows above 180 L s^{-1}, which is the theoretical maximum flow admitted to the WWTP for treatment. This limit is respected in the model, even though there are flow observations higher than 180 L s^{-1} in the sewer.

At Luppmenstrasse, the models tend to underestimate the flows (Fig. 3a). The CB leads to NSE values over the acceptable threshold (>0.5), but this is not the case for the BC. Unfortunately, any improvement in the representation of the Luppementrasse flows in the model leads to poorer performance at the WWTP node (see **SI S6**). This trade-off in model performance, which has been previously reported, could be due to several reasons, such as throttles suppressing the effect of rainfall-runoff downstream, limitations in measuring in the main collector only, and uncertainty in the collected data (Wani et al., 2022).

Table 1
Summary of relevant SWMM parameters of GSI elements for surface, soil, storage, and underdrain layers. The numbers in the parentheses illustrate the source of the parameter values, where (1) is Joshi et al. (Joshi et al., 2021), (2) is Rossman and Huber (Rossman and Huber, 2016) and (3) is Wang et al. (Wang et al., 2019). Revised values introduced by the authors based on literature and the SWMM manual are shown with an asterisk (*). The parameters of the layers that are not required by the specific GSI type in the model are shown as N/A (Not Applicable). The complete list of GSI parameters is summarised in Table S6 in SI S5.

Layer	Parameter [unit]	Bioretention basin	Permeable pavement	Green roof
Surface/ Pavement	Berm height [mm]/ Thickness pavement [mm]	150*	150 (3)	50*
	Roughness (Manning's n) [-]	0.2 (1)	0.012 (1)	0.2 (1)
	Permeability [mm h^{-1}]	N/A	500 (3)	N/A
Soil	Thickness [mm]	600 (3)	N/A	150 (3)
	Porosity [-]	0.5 (3)	N/A	0.45 (2)
	Conductivity [mm h^{-1}]	250 (3)	N/A	120*
Storage/ Drainage Mat	Thickness [mm]	150 (2)	300 (3)	75 (3)
	Seepage factor [mm h^{-1}]	7 (3)	7 (3)	N/A
Underdrain	Flow coefficient [mm h^{-1}]	0.5*	0.5 (3)	N/A

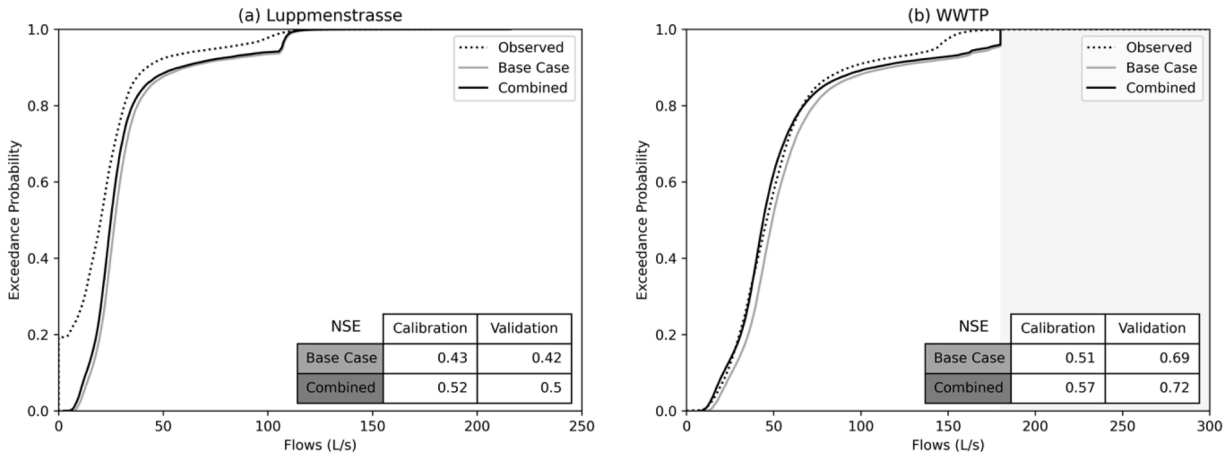

Fig. 3. Cumulative distribution curves of the observed and simulated flows considering both calibration and validation periods at (a) Luppmenstrasse (F08) and (b) the wastewater treatment plant (WWTP) (F00). Refer to Fig. 2 for their location in the catchment. The tables show the Nash-Sutcliffe Efficiency coefficient (NSE) values obtained for the calibration and validation period. In (b), the grey region highlights values higher than 180 L/s (maximum flow admitted in the WWTP).

Following a commonly adopted approach in the literature, this calibration uses flow and groundwater measurements. This is due to the limited availability of CSO volume and duration data. Our assumption is that by improving flow prediction performance, as indicated by the performance metrics, the model is able to reliably predict CSO discharges. This approach is widely used in the literature (James, 2005; Joshi et al., 2021). It may be possible to further improve the calibration by collecting CSO data with sensors, as well as, selecting other optimisation algorithms and spatially changing the subcatchment and GW parameters. However, further calibration of the model may only result in marginal improvements. For instance, the addition of the GW model led to issues in calibration, as several iterations were needed to obtain stable flows of GW in the system (related to seepage and conductivity parameters). Yet the addition of GW led to minimal change in model performance, as can be seen in Fig. 3 (combined model performs nearly the same as BC). Thus, for the authors, the advantage of including GW modelling does not lie in improved overall model performance, but in the ability to account for the dynamic interaction between GW and the sewers. However, this advantage may be less useful in SWMM due to the limitations in the SWMM GW module (e.g., the lumped nature of the modelled aquifers) (Zhang et al., 2018).

3.2. *Comparison of the different model structures*

Fig. 4 presents a comparison of how an accurate representation of different hydrological processes and water flows affects simulated estimates of annual CSO volume, duration, and frequency at the system level (without GSI). The figure also highlights whether inclusion of these processes can significantly affect results (shown as letters on top of the boxplot, where the same letter indicates that the results do not statistically significantly differ; see also **Fig. S7** in **SI S7**). As expected, the inclusion of boundary flows increases the simulated CSO volume (by up to 40 %), since more water is entering the sewer system. CSO duration and frequency also increase due to the higher catchment residence time

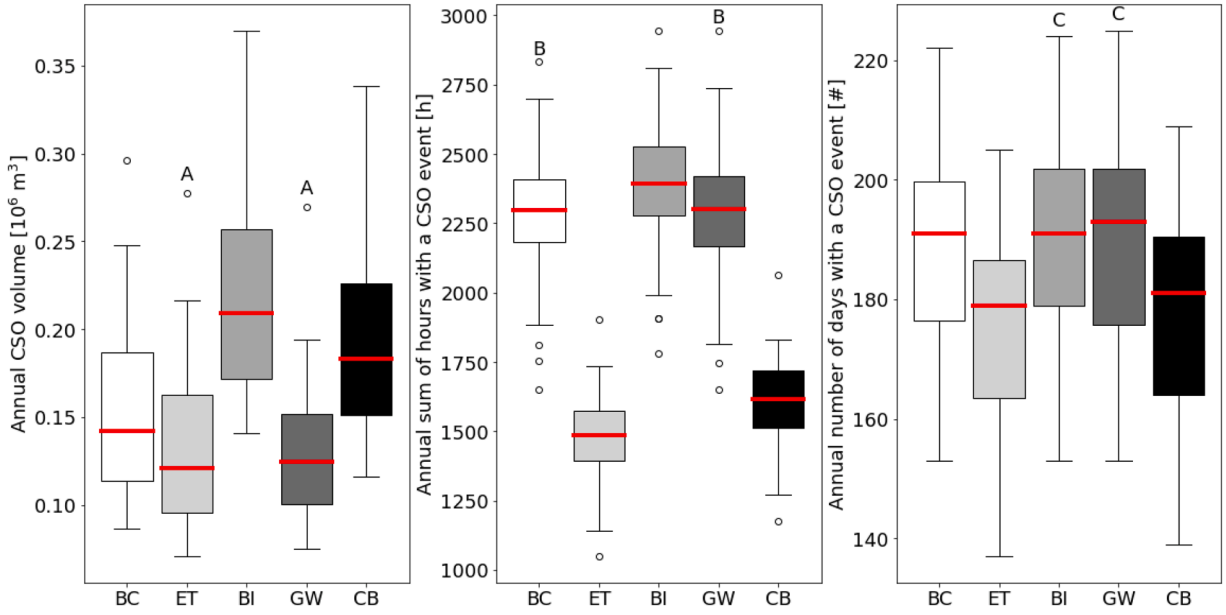

Fig. 4. Annual CSO volume (left), duration (middle), and frequency (right) for the base-case (BC), evapotranspiration (ET), boundary inflows (BI), groundwater (GW) and combined (CB) model versions without GSI. The boxplots represent the variability of the 30 years of simulations, where the box covers the central 50 % of the distribution. The whiskers span from the minimum and maximum values within the 99 % range. The red line represents the median of the annual values, while black circles are the outliers. The boxplots with the same letter on top do not differ significantly from each other, according to the results of the dependent *t*-test.

(the flows in the sewer pipes include not only wastewater but also stormwater from neighbouring municipalities, prolonging individual CSO events). When BI are included, results are always statistically significantly different from the BC.

Including ET as a time series in the simulations decreases CSO volume significantly; a median reduction of 15 % with respect to the base case model. ET is also the only model structure that reduces the duration and frequency of CSO events since surface ET reduces runoff and infiltration in the soil and thus consequently lowers the runoff volume that enters the sewer system. Small CSO emissions are avoided at the beginning or end of storm events with respect to the BC.

The inclusion of GW modelling has a negligible influence on annual CSO duration and frequency, but does significantly decrease CSO volume. The CSO volume reductions obtained with the inclusion of GW are, however, not significantly different from those of ET, indicating that the influence of ET and GW within the model is similar. The minimal (not significantly different) effect of GW on CSO duration is due to the different timescales of water flowing into the pipes from the GW module. During a storm event, water is "stored" in the GW module. Some of this water is deeply percolated, while the rest infiltrates into the sewer pipes after the storm event (defined by the rates of the groundwater and aquifer modules in SWMM, see **SI S3**). The deep percolation and the time lag between the start of the rainfall and the rise in the GW table reduce the peak CSO discharge and as a result, CSO volume decreases by 10 %, on average. At the catchment scale, more water flows from the sewer to the GW aquifer than water out of the aquifer into the pipe. Thus, the GW table is primarily below the pipes in most subcatchments; however, relevant spatial variations exist (see Section 3.4 for spatial analysis).

When ET, BI and GW processes are collectively evaluated (in the CB model), results are always significantly different from individual inclusion of these processes, indicating that individual model versions cannot predict the impact of combined hydrological processes on CSO

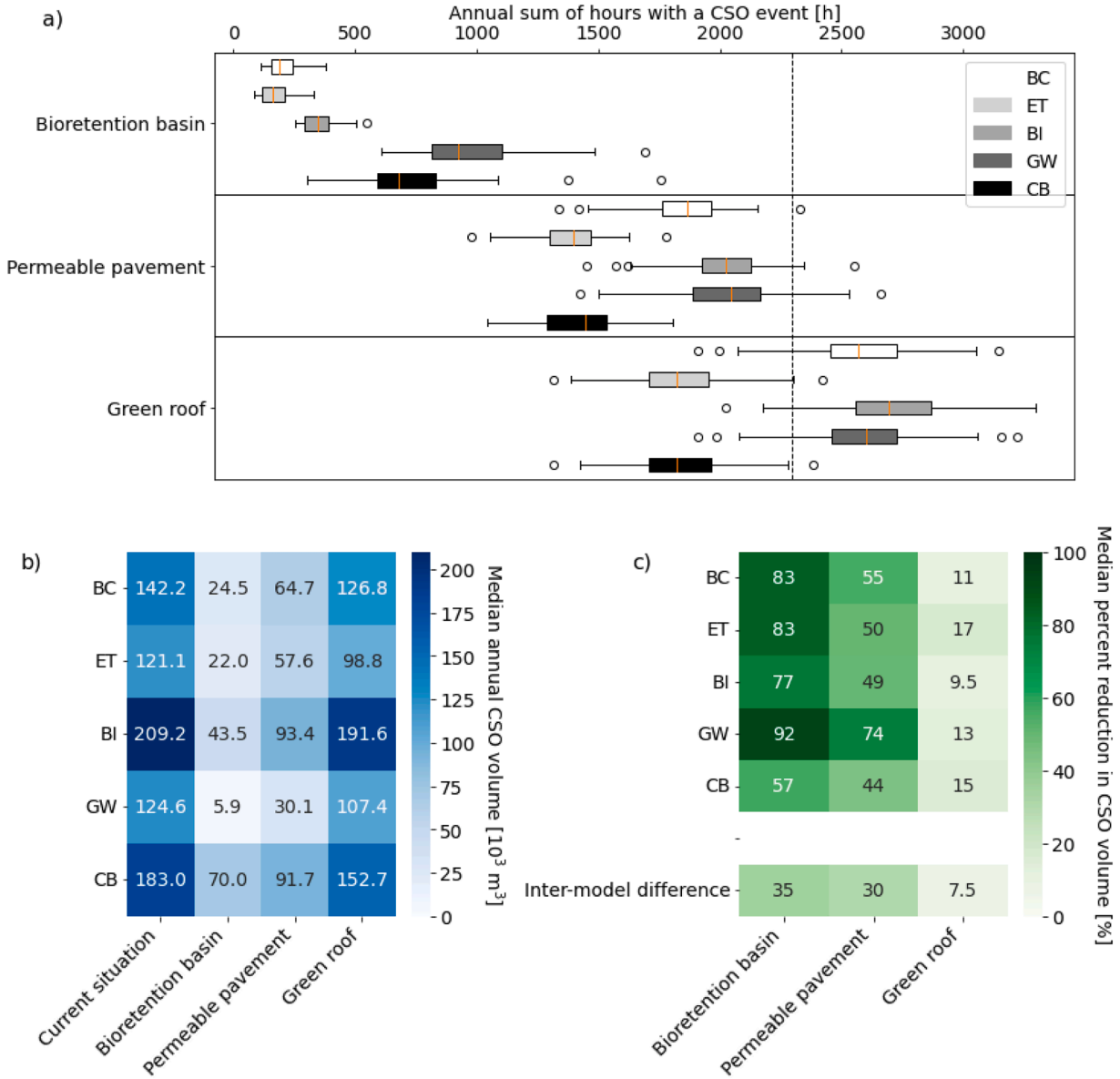

Fig. 5. The effectiveness of GSI to reduce CSOs for the various model versions that include different flows and processes (base-case (BC), evapotranspiration (ET), boundary inflows (BI), groundwater (GW) and all combined (CB)). (a) Median annual CSO duration, where the dashed vertical line represents median annual CSO duration for the BC without GSI. The boxplots represent the variability of the 30 years of simulations, where the box covers the central 50 % of the distribution, the whiskers span from the minimum and maximum values within the 99 % range, and the black circles are the outliers. (b) Median annual CSO volume. (c) Median percent reduction in annual CSO volume when GSI are included. The last row represents the largest difference in CSO percent reduction between the model versions.

discharge. When all processes are combined, CSO volumes increase significantly compared to the BC, by 24 % on average. This rise is primarily due to the inclusion of BI, since ET and GW both individually reduce flows. When all flows are evaluated together, CSO duration and frequency are significantly different from the base case, although values are only slightly higher than when ET is considered alone. The small difference between including ET and all flows shows the relevance of ET for CSO duration, which also directly affects GW processes (as less water is available for the GW module).

Although the magnitude of underestimation will vary from catchment to catchment, these results show that the efforts to include BI, ET, and GW are relevant to estimate CSO discharges, and each process has a different magnitude effect on CSO volume and duration. This relevance is also reflected in the model validation, as the CB model also improves the predictive ability of the WWTP flows, suggesting that the inclusion of BI, ET, and GW provides more accurate simulations of CSO discharge. Interestingly, CSO volume and duration do not react in the same way to model structure changes - a decrease in volume does not automatically lead to a decrease in duration. Therefore, both volume and duration should be assessed in CSO studies. The frequency, on the other hand, commonly used in CSO analyses, follows the same behaviour as the duration and therefore only the duration will be further discussed in this manuscript.

3.3. The effect of model structure on simulated GSI effectiveness

As shown in Fig. 5, when the different model versions are used to simulate the ability of GSI to reduce CSOs, *bb* lead to the largest CSO reductions, followed by *pp* and then *gr*. These patterns, consistent with values previously reported in the literature (Jean et al., 2022; Joshi et al., 2021; Roseboro et al., 2021), remain true irrespectively of the flow (s) that are included in the model. The superior performance of *bb* can be attributed to their parameters (e.g., dimensions, routing) and location within the system. Runoff from impervious surfaces is routed to *bb*, while the other GSI only treat rain falling on the surface, which contributes to the largest reductions in duration (Fig. 5a) and volume (Fig. 5b-c) of *bb*. The results with *pp* show a comparatively moderate decrease in duration and volume with respect to the baseline without GSI. Most remarkably, *gr* tend to increase the CSO duration compared to no GSI (Fig. 5a), yet decrease the volume (Fig. 5b-c) which may be attributed to the water flowing out of the roofs taking a longer time to reach the sewer, and thus translating into a higher CSO event duration, yet lower volume.

While the relative rank in performance of the GSI elements does not change between model versions, this relative performance is less important for planning than the magnitude of change for a particular GSI element – i.e., their effectiveness to reduce CSOs. When different flow(s) are accurately represented in models, the magnitude of CSO reduction varies considerably. These differences are starkest for *bb*. When GW is evaluated alone, the model estimates that when 11 % of catchment area is covered with *bb,* these GSI could reduce CSOs by 92 % (nearly all), while when all flows are included (in the CB model), this reduction is lowered to only 57 % (nearly half) (Fig. 5c). For *pp*, effectiveness varies from 44 % to 74 %, and for *gr,* from 10 % to 17 %, depending on the model version. Unsurprisingly, the addition of BI reduces the performance of GSI, as there is more water in the system, while adding ET improves GI effectiveness, with a reduction in both CSO duration and volume compared to the BC. The inclusion of ET particularly increases effectiveness for *pp* and *gr*, since these scenarios expand the amount of pervious area and thus the potential for ET to occur (more surface water available on the subcatchments to evaporate). When all flows are combined (in the CB model), CSO duration in the *pp* and *gr* scenarios are comparable to their durations in ET module, meaning that ET is a significant component in reducing CSO duration in GSI scenarios.

These results highlight that the difference in expected effectiveness of GSI will vary considerably depending on the modelling assumptions. If a consultant or engineer is tasked with determining how much and what type of GSI would be needed to eliminate CSOs, this answer will change depending on the care taken to include different hydrological processes in the model of the combined sewer system. In fact, by ignoring the upstream inflows to the catchment and not accurately representing ET (as in previous studies, such as Joshi et al. (2021) and, Roseboro et al. (2021), one could overestimate that with both *bb* and *gr,* CSOs would be eliminated. However, when all hydrologic flows are considered (GW combined with ET and BI), which is closest to reality, *bb* plus *gr* would reduce less than 75 % of CSOs when both cover 11 % of the catchment area. As GSI continues to grow in popularity as a cost-effective tool to reduce CSOs, more assessments like these will be carried out, and decision makers need to be aware of the sensitivity of the simulations to the underlying modelling choices.

3.4. The effect of groundwater on GSI in SWMM

The GW model plays a particularly striking role in the simulated CSO volume reductions obtained with *bb* and *pp*. As more infiltration and accumulation of stormwater in the soil is possible in the GW module, the simulation results show a considerable reduction in runoff and annual CSO volume. However, the GW module does not reduce simulated CSO duration, which is comparable to those encountered in the BI structure.

This reaffirms the hypothesis that the GW module accumulates water in the soil during wet periods (see Section 3.2). During storm events, the pressure in the pipes can lead to an increased exfiltration from the sewer into the soil (Fenz et al., 2005). The water in the soil can later infiltrate again into the sewer system after the storm event, when the water level in the pipes is lower than the GW table, possibly causing longer CSO events. This can be caused by the different timescale between the stormwater routed in the sewer and the GW flows, where the lag time, which is the delay time between the incidence of water at the surface and its effect on the GW table, could be greater than one day (Bhaskar et al., 2018). This is evident in the *bb* scenario, where the GW model version shows higher CSO duration values than the BI model. In this case, the higher infiltration from the *bb* leads to a delayed accumulation of water in the GW modules, which prolongs simulated CSO durations.

When all flows are combined (in the CB model), CSO durations are within the expected range, between the ET (shortest duration) and BI (longest duration) model versions; however, simulated CSO volumes are higher than in the BI scenario, which is unexpected since the inclusion of GW and ET both reduce simulated CSOs compared to the base case GSI performance (as discussed in Section 3.2). GSI in combined model perform differently with respect to the individual model versions alone, indicating that the different processes influence each other within the model, leading to results that are different from the sum of the individual model versions. This finding can be explained by the interaction between the accumulation of water in the soil in the GW modules (due to the increased allowance for infiltration) and the higher water level in the pipes where the boundary inflows flow (discussed in the following section).

These discrepancies are particularly evident in the *bb* scenario. When *bb* are added to the catchment in the CB model, the CSO volumes are higher than in all the individual model structures. This is unexpected, as GW and ET alone both reduce CSOs. As shown in Fig. 6a, which presents the CSO volumes at each outfall for *bb*, this phenomenon can be linked to irregular behaviour at a single outfall, RUB128.

Shown in dark blue in Fig. 6a, RUB128 outfall, which is downstream of the inflow from Russikon, is responsible for about 85 % of the system's CSO volume in the CB model, while two other outfalls (RUB59 and RUB80; light blues in Fig. 6a) make up the remaining 10–15 %. Explained in the following section, this variability among CSO outfalls is due to the characteristics of the subcatchments (e.g., land use, area, width) that drain to them. For instance, subcatchments with higher imperviousness (e.g., the subcatchments draining to RUB128) will have higher runoff volumes.

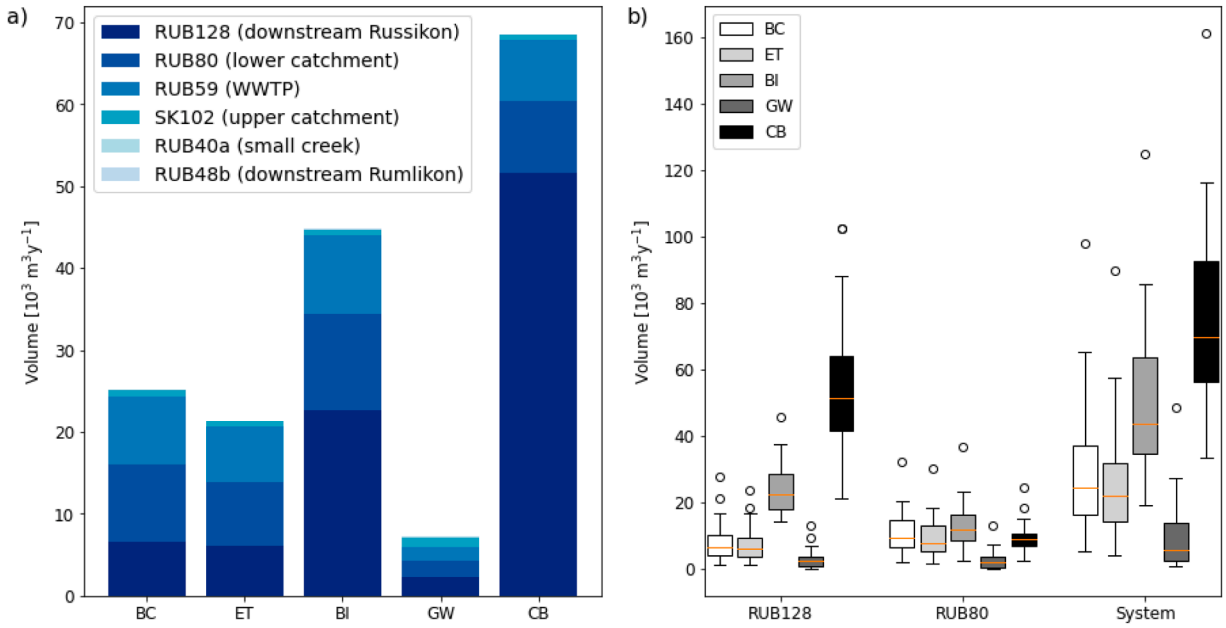

Fig. 6. (a) Annual median CSO volume at the different outfalls for the different model versions. (b) Annual CSO volumes at the most active outfalls and the system for all 30 years. The boxplots represent the variability of the 30 years of simulations, where the box covers the central 50 % of the distribution. The whiskers span from the minimum and maximum values within the 99 % range, and the black circles are the outliers.

3.5. *The bioretention basin scenario: a spatial analysis*

The higher simulated CSO volumes at RUB128 in the CB model are explained by the spatial disparity in the groundwater flows entering and exiting the sewer pipes. Fig. 7a presents the subcatchments (in blue/green) where groundwater flows *into* the sewer over the 30-year period, compared to the subcatchments (in yellow) where more water flows *out of* the pipe and into the GW aquifer. The highlighted subcatchments

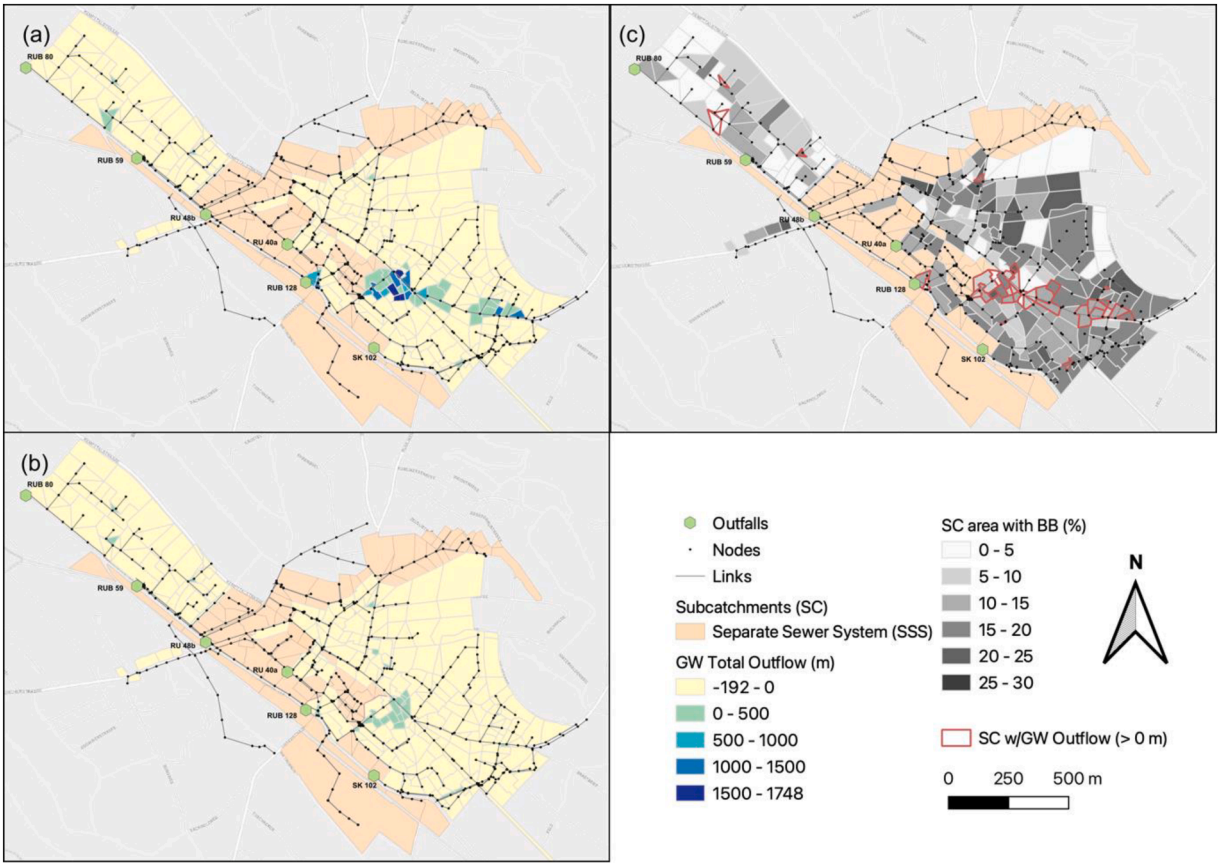

Fig. 7. Spatial analysis of the bioretention basin (*bb)* implementation. (a) Total groundwater (GW) outflows into the sewer for the combined model structure. (b) Total GW outflows into the sewer for the groundwater only structure. (c) Bioretention basin area distribution represented as the percentage of the subcatchment area.

(with infiltration into the pipes) are mostly located upstream of the RUB128 outfall, along the flow path of the main collector that routes boundary flows from Russikon. The increased CSO discharges in the CB model are a consequence of the interaction between high BI, the lumped nature of GW processes in SWMM, and the spatial distribution of the *bb*, which are highly concentrated in the upstream area contributing to RUB128 (Fig. 7c).

As mentioned in Section 3.3, the addition of *bb* delays the peak flow of water into the pipes and allows more water to accumulate in the soil in the GW modules. The boundary inflows cause CSO discharges at the beginning of a rainfall event, while the delayed flows from *bb* and the GW module lead to additional CSO discharges after the rainfall event. During storm events, due to high volumes in the sewer pipes, water exfiltrates from the sewer into the soil, since the water head in the sewer is higher than the GW table. This accumulated water in the GW modules is later released back into the sewer when the pipe is not overcharged and the GW table is higher than water head in the main collector (see **SI S8** for the head difference between the GW table and node in the different scenarios). This is also the case for water that has been infiltrated from the *bb* in the GW module, as described in Section 3.3. The spatial distribution of *bb*, their concentration in specific catchment areas, and their relationship with groundwater flows significantly influences CSO volumes, emphasising the need for a nuanced understanding of spatial dynamics when designing and implementing GSI.

Accentuating this, runoff water is delayed into the main line sewer from the *bb* in the catchments adjacent to the main line. Due to GW flowing into the pipe, the threshold for CSOs is still maintained in the sewer, leading to more CSO volume. This phenomenon is also observed in the GW-only scenario (Fig. 7b), although less accentuated as there is less water in the system due to the absence of the boundary inflows. In the GW-only model, the threshold for CSOs to happen is often not reached since the boundary inflows are not present in the pipe. This underscores the importance of considering not only the presence of GSI, but also their spatial distribution concerning the topology of the sewer system.

Overall, an accurate representation of the different hydrologic processes and flows in simulation models is crucial to determining the potential of GSI in reducing CSO duration and volume. Thus, care must be given when analysing the performance of GSI in comparison to a baseline model, as the hydrological processes included in the baseline will lead to changes in simulated effectiveness of each GSI element. At the same time, when different flows and hydrologic processes are combined during modelling, these processes can influence each other, and lead to unexpected results in GSI performance. There is ultimately a threshold of water in the sewer that will trigger CSOs and the more flows that are considered in the model, the more often this threshold will be reached. Different GSI elements contribute in different ways to reaching this threshold. This highlights the need to carefully consider the impact of modelled flows and GSI elements when designing and implementing GSI solutions for CSO mitigation.

4. Conclusions and future work

This study showed that modelling assumptions regarding hydrological processes and flows (including groundwater, evapotranspiration, and external inflows) significantly influence catchment level estimates of combined sewer overflows (CSOs) and the effectiveness of green stormwater infrastructure (GSI) to reduce them. In Fehraltorf, Switzerland, failure to include inflows from neighbouring communities in the estimation of baseline CSO conditions led to an underestimation of CSO volume by 40 %, while neglect of evapotranspiration and groundwater ended in an overestimation of CSO volume by 15 % and 10 %, respectively, on average. Neglecting these flows in baseline modelling also led to inaccurate expectations of GSI performance, despite the fact that GSI effectiveness was based on a "comparative" analysis between baseline conditions without GSI and scenarios with GSI. The expected CSO reduction due to GSI implementation varied by 35 % for bioretention basins (*bb*), 30 % for permeable pavement (*pp*), and 8 % for green roofs (*gr*), when comparing different versions of the model.

Some modelling decision require special attention, including the use of groundwater models in SWMM when green stormwater infrastructure are present. For bioretention basins, where more water is infiltrated into the groundwater, there is potential to increase CSOs at particular outflows, which is ultimately due to the characteristics of the subcatchments that feed each outfall and the interactions between the hydrological and hydraulic processes considered. Effort-to-improvement ratio should also be considered, as minor model modifications (e.g., imperviousness updates) and inclusion of boundary inflows offer high reward with minimal effort, while groundwater modules and genetic algorithm calibration demand significant effort with limited performance gains.

Overall, within combined sewer systems, the complex, interaction between different hydrologic processes and flows can lead to a range of possible CSO discharge volumes and frequencies, especially when green stormwater infrastructure are present. When hydrologic simulation models are used to estimate CSOs and effectiveness of GSI to reduce them, these complex interactions should be included to the extent possible, in particular when these estimates are used to make costly investment decisions. At the very least, baseline assumptions and associated uncertainties should be clearly stated and accounted for in all communications to inform planning and design.

As CSO measurements and GSI implementation increase in the future, the results presented here should be validated using real-world data. The models used to evaluate the effect of groundwater and GSI on combined sewer overflows could also be improved, as SWMM could be coupled with a more detailed GW model, such as MODFLOW. To better represent the complexity of urban drainage systems in these models, a variety of run-off routing and combinations of GSI types should also be considered in future studies. Future research will need also to consider how a future climate will affect CSOs and these interactions, as more water will likely flow into the system due to increases in extreme events, which can exacerbate the issues encountered with groundwater and GSI in modelling. The effect of the interactions of various hydrologic processes on CSOs should also be considered in terms of costs in order to highlight the monetary consequences of under or overestimating combined sewer overflow discharge.

Although this study did not consider the water quality aspects of combined sewer overflows and the green stormwater infrastructure, this paper is the first to identify how different hydrologic processes affect combined sewer overflows and their interaction with green stormwater infrastructure in a full-scale catchment. Accurately simulating the flows in a combined sewer system is the first step towards a better understanding the impacts of pollutants on receiving waters. In conclusion, the study cautions against the notion that baseline modelling assumptions do not matter in comparative analyses with GSI, as results show that these assumptions can considerably influence comparative GSI effectiveness.

CRediT authorship contribution statement

Mayra Rodriguez: Conceptualization, Methodology, Software, Validation, Formal analysis, Visualization, Writing – original draft, Writing – review & editing. **Giovan Battista Cavadini:** Conceptualization, Methodology, Formal analysis, Visualization, Writing – original draft, Writing – review & editing. **Lauren M. Cook:** Conceptualization, Methodology, Resources, Supervision, Project administration, Funding acquisition, Writing – review & editing.

Declaration of competing interest

The authors declare the following financial interests/personal relationships which may be considered as potential competing interests:

Giovan Battista Cavadini reports financial support was provided by Swiss National Science Foundation. Mayra Rodriguez reports financial support was provided by ETH Zurich.

Data availability

Data will be made available on request.

Acknowledgements

We acknowledge the support of the SNSF (BETTER; project 200021_204790) and Prof. Max Maurer, ETH Zurich for financing this research. We are grateful for the computing resources provided by the Euler (ETH) and CSCS cluster. We also thank the UWO project (Eawag) for providing the case-study data, the SWW team, and Stuart Dennis for their support.

Data and code availability

Data and code for the SWMM model structures described in this paper are provided open access at the following DOI: https://doi.org/10.25678/0009PE. Data and code for the original model can be found here: Blumensaat et al. (Blumensaat et al., 2023).

Supplementary materials

Supplementary material associated with this article can be found, in the online version, at doi:10.1016/j.watres.2024.121284.

References

Allen, R., Pereira, L., Raes, D., Smith, M., 1998. Crop evapotranspiration - guidelines for computing crop water requirements - FAO Irrigation and drainage paper 56, Evapotranspiración del cultivo Guías para la determinación de los requerimientos de agua de los cultivos. ESTUDIO FAO RIEGO Y DRENAJE 56. Rome.

Almaaitah, T., Appleby, M., Rosenblat, H., Drake, J., Joksimovic, D., 2021. The potential of Blue-Green infrastructure as a climate change adaptation strategy: a systematic literature review. Blue-Green Syst. 3, 223–248. https://doi.org/10.2166/bgs.2021.016.

Bai, P., Liu, X., Liang, K., Liu, C., 2015. Comparison of performance of twelve monthly water balance models in different climatic catchments of China. J. Hydrol. (Amst) 529, 1030–1040. https://doi.org/10.1016/j.jhydrol.2015.09.015.

Balmforth, D.J., 1990. The pollution aspects of storm-sewage overflows. Water Environ. J. 4, 219–226. https://doi.org/10.1111/j.1747-6593.1990.tb01382.x.

Bhaskar, A.S., Hogan, D.M., Nimmo, J.R., Perkins, K.S., 2018. Groundwater recharge amidst focused stormwater infiltration. Hydrol. Process. 32, 2058–2068. https://doi.org/10.1002/hyp.13137.

Blank, J., Deb, K., 2020. Pymoo: multi-objective optimization in python. IEEe Access. 8, 89497–89509. https://doi.org/10.1109/ACCESS.2020.2990567.

Blumensaat, F., Bloem, S., Ebi, C., Disch, A., Förster, C., Maurer, M., 2021. "The urban water observatory-long-term monitoring of urban water resources dynamics in very high spatiotemporal resolution using low-power sensor and data communication techniques [W.W.W Document]. URL https://uwo-opendata.eawag.ch/(accessed 5.6.22).

Blumensaat, F., Bloem, S., Ebi, C., Disch, A., Förster, C., Maurer, M., Rodriguez, M., Rieckermann, J., 2023. The UWO dataset-long-term data from a real-life field laboratory to better understand urban hydrology at small spatiotemporal scales. Pre-Print.

Broekhuizen, I., Muthanna, T.M., Leonhardt, G., Viklander, M., 2019. Urban drainage models for green areas: structural differences and their effects on simulated runoff. J. Hydrol. X. 5, 100044 https://doi.org/10.1016/j.hydroa.2019.100044.

Browder, G., Ozment, S., Rehberger Bescos, I., Gartner, T., Lange, G.-M., 2019. Integrating Green and Gray: Creating Next Generation Infrastructure. WRI Publications. https://doi.org/10.46830/wrirpt.18.00028.

Butler, D., Digman, C., Makropoulos, C., Davies, J., 2018. Urban Drainage, Fourth. ed, Urban Drainage. Taylor & Francis, Boca Raton, United States. https://doi.org/10.4324/9780203351673.

Calanca, P., Smith, P., Smith, Pascalle, Holzkämper, A., Ammann, C., 2011. Die Referenzverdunstung und ihre Anwendung in der Agrarmeteorologie. Agrarforsch Schweiz 2, 176–183.

Casal-Campos, A., Fu, G., Butler, D., Moore, A., 2015. An integrated environmental assessment of green and gray infrastructure strategies for robust decision making. Environ. Sci. Technol. 49, 8307–8314. https://doi.org/10.1021/es506144f.

Chatzimentor, A., Apostolopoulou, E., Mazaris, A.D., 2020. A review of green infrastructure research in Europe: challenges and opportunities. Landsc. Urban. Plan. 198, 103775 https://doi.org/10.1016/j.landurbplan.2020.103775.

Cook, L.M., Larsen, T.A., 2021. Towards a performance-based approach for multifunctional green roofs: an interdisciplinary review. Build. Environ. 188, 107489 https://doi.org/10.1016/j.buildenv.2020.107489.

Cook, L.M., Samaras, C., VanBriesen, J.M., 2018. A mathematical model to plan for long-term effects of water conservation choices on dry weather wastewater flows and concentrations. J. Environ. Manage 206, 684–697. https://doi.org/10.1016/j.jenvman.2017.10.013.

Copetti, D., Marziali, L., Viviano, G., Valsecchi, L., Guzzella, L., Capodaglio, A.G., Tartari, G., Polesello, S., Valsecchi, S., Mezzanotte, V., Salerno, F., 2019. Intensive monitoring of conventional and surrogate quality parameters in a highly urbanized river affected by multiple combined sewer overflows. Water. Sci. Technol. Water. Supply. 19, 953–966. https://doi.org/10.2166/ws.2018.146.

Deb, K., Pratap, A., Agarwal, S., Meyarivan, T., 2002. A fast and elitist multiobjective genetic algorithm: NSGA-II. IEEE Trans. Evol. Comput. 6, 182–197. https://doi.org/10.1109/4235.996017.

Deletic, A., Dotto, C.B.S., McCarthy, D.T., Kleidorfer, M., Freni, G., Mannina, G., Uhl, M., Henrichs, M., Fletcher, T.D., Rauch, W., Bertrand-Krajewski, J.L., Tait, S., 2012. Assessing uncertainties in urban drainage models. Physics and chemistry of the earth, estimating and representing uncertainty in applied hydrology, hydraulics and water quality studies 42–44, 3–10. https://doi.org/10.1016/j.pce.2011.04.007.

De-Ville, S., Stovin, V., 2023. Predicting Bioretention evapotranspiration from meteorological, mass-loss, and moisture-loss data, in: Novatech 2023 11e Conférence Internationale Sur l'eau Dans La Ville. Lyon, France.

DHI, 2023. MIKE - Powered by DHI [WWW Document]. URL https://www.mikepoweredbydhi.com/products/new-features (accessed 2.27.23).

Ebrahimian, A., Wadzuk, B., Traver, R., 2019. Evapotranspiration in green stormwater infrastructure systems. Sci. Total Environ. 688, 797–810. https://doi.org/10.1016/j.scitotenv.2019.06.256.

Environment Agency, Department for Environment, F.& R.A., 2022. Improved Monitoring of Sewage Spills to Drive Enhanced Environmental Protection and Enforcement - GOV.UK [WWW Document]. URL https://www.gov.uk/government/news/improved-monitoring-of-sewage-spills-to-drive-enhanced-environmental-protection-and-enforcement (accessed 5.16.22).

Federal Office for Statistics, S., 2022. Ständige Wohnbevölkerung nach Staatsangehörigkeitskategorie, Geschlecht und Gemeinde, Provisorische Jahresergebnisse, 2021 - 2021 | Tabelle | Bundesamt für Statistik [W.W.W Document]. URL https://www.bfs.admin.ch/bfs/de/home/statistiken/kataloge-datenbanken/tabellen.assetdetail.21826815.html (accessed 5.5.22).

Fenz, R., Blaschke, A.P., Clara, M., Kroiss, H., Mascher, D., Zessner, M., 2005. Quantification of sewer exfiltration using the anti-epileptic drug carbamazepine as marker species for wastewater. Water Sci. Technol. 52, 209–217. https://doi.org/10.2166/wst.2005.0321.

Figueroa, A., Hadengue, B., Leitão, J.P., Rieckermann, J., Blumensaat, F., 2021. A distributed heat transfer model for thermal-hydraulic analyses in sewer networks. Water. Res. 204 https://doi.org/10.1016/j.watres.2021.117649.

Fischbach, J., Siler-Evans, K., Tierney, D., Wilson, M., Cook, L., May, L., 2017. Robust Stormwater management in the pittsburgh region: a pilot study, robust stormwater management in the pittsburgh region: a pilot study. RAND Corp. https://doi.org/10.7249/rr1673.

Freedman, D., Pisani, R., Purves, R., 2007. Statistics, 4th Editio. ed. WW Norton & amp, Company, New York.

Fu, X., Goddard, H., Wang, X., Hopton, M.E., 2019. Development of a scenario-based stormwater management planning support system for reducing combined sewer overflows (CSOs). J. Environ. Manage 236, 571–580. https://doi.org/10.1016/j.jenvman.2018.12.089.

Hadengue, B., Joshi, P., Figueroa, A., Larsen, T.A., Blumensaat, F., 2021. In-building heat recovery mitigates adverse temperature effects on biological wastewater treatment: a network-scale analysis of thermal-hydraulics in sewers. Water. Res. 204, 117552 https://doi.org/10.1016/j.watres.2021.117552.

Hörnschemeyer, B., Henrichs, M., Uhl, M., 2021. Swmm-urbaneva: a model for the evapotranspiration of urban vegetation. Water (Switzerland) 13, 243. https://doi.org/10.3390/w13020243.

Hung, F., Harman, C.J., Hobbs, B.F., Sivapalan, M., 2020. Assessment of climate, sizing, and location controls on green infrastructure efficacy: a timescale framework. Water. Resour. Res. 56 https://doi.org/10.1029/2019WR026141.

Innovyze, 2014. Sanitary Sewer Modeling Software | InfoWorks ICM sewer edition [W.W.W Document]. URL https://www.innovyze.com/en-us/products/infoworks-icm-se (accessed 6.4.22).

James, W., 2005. Rules for Responsible Modeling, 4th Edition. Computational Hydraulic International Press (CHI), Guelph, Ontario, Canada. ISBN 978-0-9683681-5-2.

Jean, M., Morin, C., Duchesne, S., Pelletier, G., Pleau, M., 2022. Real-time model predictive and rule-based control with green infrastructures to reduce combined sewer overflows. Water. Res. 221, 118753 https://doi.org/10.1016/j.watres.2022.118753.

Joshi, P., Leitão, J.P., Maurer, M., Bach, P.M., 2021. Not all SuDS are created equal: impact of different approaches on combined sewer overflows. Water. Res. 191 https://doi.org/10.1016/j.watres.2020.116780.

Keller, C., 2016. Understanding the urban drainage system of Fehraltorf Enhancing the reliability of Fehraltorf's SWMM model through calibration.

Kim, Y., Chester, M.V., Eisenberg, D.A., Redman, C.L., 2019. The infrastructure trolley problem: positioning safe-to-fail infrastructure for climate change adaptation. Earths. Future 7, 704–717. https://doi.org/10.1029/2019EF001208.

Krejci, V., Schilling, W., Gammeter, S., 1994. Receiving water protection during wet weather vladimir Krejci, Wolfgang Schilling and Sonja Gammeter. Water Sci. Technol. 29, 219–229.
Leimgruber, J., Krebs, G., Camhy, D., Muschalla, D., 2018. Sensitivity of model-based water balance to low impact development parameters. Water (Switzerland) 10, 1838. https://doi.org/10.3390/w10121838.
Li, C., Peng, C., Chiang, P.C., Cai, Y., Wang, X., Yang, Z., 2019. Mechanisms and applications of green infrastructure practices for stormwater control: a review. J. Hydrol. (Amst) 568, 626–637. https://doi.org/10.1016/j.jhydrol.2018.10.074.
Maier, H.R., Dandy, G.C., 2000. Neural networks for the prediction and forecasting of water resources variables: a review of modelling issues and applications. Environ. Modell. Softw. 15, 101–124. https://doi.org/10.1016/S1364-8152(99)00007-9.
Matsler, A.M., Meerow, S., Mell, I.C., Pavao-Zuckerman, M.A., 2021. A 'green' chameleon: exploring the many disciplinary definitions, goals, and forms of "green infrastructure. Landsc. Urban. Plan. 214, 104145 https://doi.org/10.1016/j.landurbplan.2021.104145.
McDonnell, B., Ratliff, K., Tryby, M., Wu, J., Mullapudi, A., 2020. PySWMM: the python interface to Stormwater management model (SWMM). J. Open. Source Softw. 5, 2292. https://doi.org/10.21105/joss.02292.
Moriasi, D.N., Arnold, J.G., Van Liew, M.W., Bingner, R.L., Harmel, R.D., Veith, T.L., 2007. Model evaluation guidelines for systematic quantification of accuracy in watershed simulations. Trans. ASABe 50, 885–900.
Niazi, M., Nietch, C., Maghrebi, M., Jackson, N., Bennett, B.R., Tryby, M., Massoudieh, A., 2017. Storm water management model: performance review and gap analysis. J. Sustain. Water. Built. Environ. 3, 4017002 https://doi.org/10.1061/jswbay.0000817.
Passerat, J., Ouattara, N.K., Mouchel, J.M., Rocher, Vincent, Servais, P., 2011. Impact of an intense combined sewer overflow event on the microbiological water quality of the Seine River. Water. Res. 45, 893–903. https://doi.org/10.1016/j.watres.2010.09.024.
Philadelphia Water Department, 2023. Stormwater Management Guidance Manual.
Ramgraber, M., Weatherl, R., Blumensaat, F., Schirmer, M., 2021. Non-gaussian parameter inference for hydrogeological models using stein variational gradient descent. Water. Resour. Res. 57 (21) https://doi.org/10.1029/2020WR029339 e2020WR029339.
Roseboro, A., Torres, M.N., Zhu, Z., Rabideau, A.J., 2021. The impacts of climate change and porous pavements on combined sewer overflows: a case study of the City of Buffalo, New York, USA. Front. Water. 3, 110. https://doi.org/10.3389/frwa.2021.725174.
Rossman, L.A., 2015. Storm Water Management Model User's Manual Version 5.1. U.S. Environmental Protection Agency.
Rossman, L.A., Huber, W.C., 2016a. Storm Water Management Model Reference Manual Volume I – Hydrology (revised)(EPA/600/R-15/162A). U.S. Environmental Protection Agency I, p. 231.
Rossman, L.A., Huber, W.C., 2016b. Storm Water Management Model Reference Manual Volume III - Water Quality. Environmental Protection III, p. 158.
Scikit-Learn Developers, 2014. 1.17. Neural network models (supervised) — Scikit-learn 1.2.1 documentation [W.W.W Document]. URL https://scikit-learn.org/stable/modules/neural_networks_supervised.html (accessed 2.27.23).
Staufer, P., Scheidegger, A., Rieckermann, J., 2012. Assessing the performance of sewer rehabilitation on the reduction of infiltration and inflow. Water. Res. 46, 5185–5196. https://doi.org/10.1016/J.WATRES.2012.07.001.
The SciPy Community, 2023. SciPy v1.11.3 Manual.
Torres, M.N., Fontecha, J.E., Walteros, J.L., Zhu, Z., Ahmed, Z., Rodríguez, J.P., Rabideau, A.J., 2021. City-scale optimal location planning of Green Infrastructure using piece-wise linear interpolation and exact optimization methods. J. Hydrol. (Amst) 601. https://doi.org/10.1016/j.jhydrol.2021.126540.
U.S.C, 2020. Wet Weather Quality Act of 2000.
Wang, M., Sweetapple, C., Fu, G., Farmani, R., Butler, D., 2017. A framework to support decision making in the selection of sustainable drainage system design alternatives. J. Environ. Manage 201, 145–152. https://doi.org/10.1016/j.jenvman.2017.06.034.
Wang, M., Wang, Y., Gao, X., Sweetapple, C., 2019. Combination and placement of sustainable drainage system devices based on zero-one integer programming and schemes sampling. J. Environ. Manage 238, 59–63. https://doi.org/10.1016/j.jenvman.2019.02.129.
Wani, O., Ph, D., Maurer, M., Ph, D., Rieckermann, J., Ph, D., Blumensaat, F., 2022. Does distributed monitoring improve the calibration of urban drainage models ?. In: 12th Urban Drainage Modeling Conference.
Weiß, G., Brombach, H., Haller, B., 2002. Infiltration and inflow in combined sewer systems: long-term analysis. Water Sci. Technol. 45, 11–19. https://doi.org/10.2166/WST.2002.0112.
Zhang, K., Chui, T.F.M., 2020. Assessing the impact of spatial allocation of bioretention cells on shallow groundwater – an integrated surface-subsurface catchment-scale analysis with SWMM-MODFLOW. J. Hydrol. (Amst) 586, 124910. https://doi.org/10.1016/j.jhydrol.2020.124910.
Zhang, K., Chui, T.F.M., Yang, Y., 2018. Simulating the hydrological performance of low impact development in shallow groundwater via a modified SWMM. J. Hydrol. (Amst) 566, 313–331. https://doi.org/10.1016/j.jhydrol.2018.09.006.